

SACLANTCEN MEMORANDUM

serial no.: SM-241

*SACLANT UNDERSEA
RESEARCH CENTRE*

MEMORANDUM



**Model statistics of inertial shear
from multi-year simulations
at weathership 'Mike'**

L. Henderson
and S. Piacsek

December 1990

The SACLANT Undersea Research Centre provides the Supreme Allied Commander Atlantic (SACLANT) with scientific and technical assistance under the terms of its NATO charter, which entered into force on 1 February 1963. Without prejudice to this main task – and under the policy direction of SACLANT – the Centre also renders scientific and technical assistance to the individual NATO nations.

This document is released to a NATO Government at the direction of SACLANT Undersea Research Centre subject to the following conditions:

- The recipient NATO Government agrees to use its best endeavours to ensure that the information herein disclosed, whether or not it bears a security classification, is not dealt with in any manner (a) contrary to the intent of the provisions of the Charter of the Centre, or (b) prejudicial to the rights of the owner thereof to obtain patent, copyright, or other like statutory protection therefor.
- If the technical information was originally released to the Centre by a NATO Government subject to restrictions clearly marked on this document the recipient NATO Government agrees to use its best endeavours to abide by the terms of the restrictions so imposed by the releasing Government.

Page count for SM-241
(excluding covers)

Pages	Total
i-vi	6
1-23	23
	<hr/>
	29

SACLANT Undersea Research Centre
Viale San Bartolomeo 400
19026 San Bartolomeo (SP), Italy

tel: 0187 540 111
fax: 0187 524 600
telex: 271148 SACENT I

NORTH ATLANTIC TREATY ORGANIZATION


SACLANTCEN SM-241

Model statistics of
inertial shear from
multi-year simulations
at weathership 'Mike'

L. Henderson and S. Piacsek

The content of this document pertains
to work performed under Project 04 of
the SACLANTCEN Programme of Work.
The document has been approved for
release by The Director, SACLANTCEN.

Issued by:
Underwater Research Division



J.M. Hovem
Division Chief

SACLANTCEN SM-241

**Model statistics of inertial shear
from multi-year simulations at
weathership 'Mike'**

L. Henderson and S. Piacsek

Executive Summary: Recently there has been increased interest in ASW-related environmental acoustics research on the influence of the oceanic fine-structure and internal waves on acoustic signal propagation. Both the direct source mechanisms that generate such structures and fluctuations, as well as the environmental factors that affect their propagation and/or dissipation, are of direct interest to applied oceanographic research.

This memorandum focuses on one of the most important environmental factors affecting the propagation and dissipation of internal waves: the presence of strong vertical shear in the mean currents. It has been known for a long time by fluid dynamicists and oceanographers that in such a current shear the internal waves suffer critical layer absorption and strong refraction, thus strongly influencing their spectra and level of activity in a given region.

At the base of the mixed layer the main contribution to vertical current shears comes from inertial currents generated by strong winds, and from breaking internal waves. (The latter phenomena is not independent of the presence of the former.)

Using a numerical model for the turbulent surface mixed layer, we have investigated two aspects of inertial shear statistics: the interannual variations due to variability of the atmospheric forcing fluxes, and the sensitivity of the model-predicted shear to the grid size employed in the prediction model.

The results have shown that there are strong interannual variations in the magnitude and predominant depth of inertial shear, with magnitudes varying by a factor of up to three, and the depth of mean shear moving by 30 m or more. A dependence of these quantities on the vertical grid size has also been found, with the simulation results showing large inaccuracies for $\delta z > 5$ m. In particular, this implies that the current TOPS (thermal ocean prediction system) operational model can predict inertial shear statistics only marginally at best.

This work was part of a larger study of upper ocean shear funded by NORDA, and satisfied our contract requirements. No further work on this topic by SACLANTCEN is planned.

**Model statistics of inertial shear
from multi-year simulations at
weathership 'Mike'**

L. Henderson and S. Piacsek

Abstract: In this memorandum we focus on one of the most important environmental factors affecting the propagation and dissipation of internal waves: the presence of strong vertical shear in the mean currents. Using a numerical model for the turbulent surface mixed layer, we have investigated two aspects of inertial shear statistics: the interannual variations due to variability of the atmospheric forcing fluxes, and the sensitivity of the model predicted shear to the grid size employed in the prediction model. To study the interannual variation of shear, we performed a simulation for the month of May for 20 consecutive years from 1960–1979 at the site of weathership 'Mike' in the Norwegian Sea. To examine the dependence of the shear statistics on the vertical grid size, we performed the computations on grid sizes of 1 m, 2 m, 5 m, and a grid approximating the TOPS grid (for the top 100 m). The results show that there are strong interannual variations in the magnitude and predominant depth of inertial shear, with magnitudes varying by a factor of up to three, and the depth of maximum shear moving by 30 m or more. A dependence of these quantities on the vertical grid size is also found, with the simulation results showing large inaccuracies for δz greater than 5 m.

Keywords: atmospheric forcing ◦ currents ◦ inertial shear ◦ internal waves ◦ mixed layer ◦ Norwegian Sea

Contents

1. Importance of shear	1
2. Nature of shear	2
3. Scope of present work	4
4. Model description	5
5. Initialization and forcing	7
6. Statistical method and output display	11
7. Discussion of results	12
8. Conclusions	21
References	22

Acknowledgement: The authors would like to thank Dr. Paul Martin for supplying the forcing functions at weathership 'Mike' and the original version of the Mellor-Yamada model. The authors are also indebted to Mr. Pim van Meurs for preparing some of the plotting routines.

1

Importance of shear

This study is a continuation of a research effort to evaluate the capability of the current FNOC (Fleet Numerical Oceanographic Center) ocean forecast model TOPS (Thermal Ocean Prediction System) to predict some of the environmental parameters that are of interest to acoustic and non-acoustic ASW. One of these parameters is the vertical shear of the horizontal velocity, shown by both observational and theoretical work to have a strong effect on the propagation of internal waves, and on the generation and evolution of turbulent patches and fine structure in the ocean.

The largest shears in the ocean are usually associated with inertial waves and breaking internal waves, and are found in many cases near the surface or near the bottom of the mixed layer. Since it is impossible to measure or monitor experimentally the velocity shear associated with these motions over large areas of the world ocean, one has to have recourse to numerical models. The highly intermittent nature of velocity shear, however, makes a deterministic prediction very difficult if not impossible. What has been considered and attempted so far is a simulation of certain statistical aspects of these motions, including spectral slopes and intensity levels of activity, and their dependence on season, geography, and/or the mesoscale flow.

Important factors that influence the prediction problem are the accuracy of the forcing functions, the representation of all the physical phenomena present, and various aspects of the numerical model, among them the size of the spatial grid on which the variables are defined.

2

Nature of shear

The nature of inertial shear has been investigated by many authors in the last few years, both experimentally and numerically. The various observational studies have found the maximum shear values to range from 0.002 to 0.1 s⁻¹, although most maxima tend to fall between 0.01 to 0.04 s⁻¹. The observations most often find the maximum shear to occur near and below the base of the mixed layer (Gregg and Sanford, 1980; Davis et al., 1981a; Oakey, 1982; Oakey and Elliot, 1982; Rubenstein and Newman, 1982; D'Asaro and Sanford, 1981; Briscoe and Weller, 1984). Several investigators have found evidence that the motions below the mixed layer are not driven directly by the local wind.

These observations tend to be confirmed on the whole also by numerical simulation studies (Davis et al., 1981b; Martin, 1982; Martin et al., 1986). Recent observational evidence for the shear frequency and vertical wave-number spectrum in the upper ocean has been produced by Pinkel (1984). He has shown that the variance of shear in the inertial-period band occurs in vertical scales of tens of meters, and that there is a rapid fall-off of shear with decreasing vertical scales. In the frequency band corresponding to the Brunt-Väisälä period, the smallest vertical scales contribute the most to the variance, and the shear spectrum is white with respect to vertical scales. Pinkel's observational picture is in sharp contrast with the shear spectrum model derived from the internal wave model of Garrett and Munk (1972, 1975), or any other semi-empirical model. These models predict that most of the variance of shear should occur at the inertial frequency, but Pinkel's observations refute it by pointing out that only about half of the shear variance is captured by motions at the inertial frequency. Pinkel's observations did not single out the mixed layer as a special region for shear. This memorandum addresses that fraction of the shear variance that is generated by the inertial motions at the base of the mixed layer.

In model studies with a constant wind stress (Warn-Varnas et al., 1981b), it was found that the amplitude of the inertial velocity becomes constant throughout the mixed-layer depth and zero below the mixed layer, leading to the formation of maximum shears near the bottom of the mixed layer and near the surface. Since the shear within and at the base of the mixed layer is due largely to currents that are directly wind-driven, the shear in this region tends to be correlated with the surface forcing rather well. When the maximum shear occurs below the base of the mixed layer, the situation corresponds to one where stresses due to growing winds are superimposed on a previously oscillating inertial wave.

SACLANTCEN SM-241

These analyses were performed by decomposing the velocity into an Ekman and inertial part. The Ekman part of the shear was found to be dependent upon the instantaneous wind stress at the surface, while the inertial part was influenced by present and past wind stresses. Once an inertial wave was excited, it remained present for ca. 10 days till it was damped out, whereas the Ekman part of the velocity diminished to zero as the wind stress decreased to zero.

In a simulation of the MILE (Mixed Layer Experiment) experiment carried out in 1977, one of the most comprehensive studies of mixed-layer dynamics up to that time (Davis et al., 1981a; Levine et al., 1983), Martin et al. (1986) found that the currents in the upper 15–20 m were primarily driven by the local winds. Between 20 and 30 m the motions were thought likely to be due to a mixture of both local wind-driving and dispersion. Below 30 m the motions were proposed to be caused primarily by dispersion, since vertical mixing did not extend to those depths.

The formation of vertical shear both within and below the mixed layer has also been investigated in connection with MILE simulations. In the upper 20 m or so, the predicted shear agreed well with the observed shear, and it was found to be closely influenced by the surface forcing. Between 20 and 30 m, however, the model-predicted shear increased only during the stronger wind events, which deepened the mixed layer to these depths. Furthermore, the observed shear showed much more variability on the shorter timescales, possibly caused by phenomena not included in the model (e.g. internal waves). Below 30 m, the maximum observed mixed-layer depth during MILE, the model predicted almost no shear, whereas the observations showed considerable shear present between 30 and 50 m, within the seasonal thermocline.

In general, four main timescales of the atmospheric forcing functions have been found to affect the formation of shear: the diurnal heating/cooling cycle, the 3–7 day random procession of fronts and storms, the seasonal cycle, and an annual variation in the frequency and intensity of storms. Harding et al. (1983) found that high shear variability appears on diurnal, synoptic, and interannual time scales. Further studies along these lines, with similar findings, were performed by Preller and Piacsek (1985), Warn-Varnas et al. (1986), and Piacsek et al. (1988).

3

Scope of present work

In order to gain an insight into the interannual variation of shear, we have performed a simulation for the month of May for 20 consecutive years from 1960–1979, at the site of weathership ‘Mike’ in the Norwegian Sea, located at 66°N, 2°E. In order to examine the dependence of the shear statistics on the vertical grid size, we have performed the computations on grid sizes of 1, 2, 5 m, and a grid approximating the TOPS grid for the top 100 m.

In summary, the current work was mainly designed to serve as a sensitivity study for estimating the dependence of the modeled shear on the grid size and on the variations in the forcing functions. It was not designed to be compared with observational data, and as such was not initialized, updated and verified against XBT and/or current meter observations.

A second goal of the study was to make a first-order estimate of the adequacy of the operational TOPS model to predict shear. By request of NORDA the velocity fields from the daily output of TOPS have also been archived (in addition to temperature and salinity), and for the year 1985 several studies have been made using these fields (Warn-Varnas et al., 1986; Piacsek et al., 1988) to derive the statistics of the various environmental parameters, including shear. A comparison of the two model shear statistics is attempted.

Model description

The mixed-layer model used in this study is a 'profile' or 'differential' type model, in which all the physical variables are defined on a fixed vertical set of grid points, and their time evolution computed via transport equations in finite-difference form. The vertical variation of the variables and their time changes can be followed to any desired accuracy by choosing a fine enough spatial grid and small enough time step.

In contrast, 'bulk' type models assume the existence of a mixed layer a priori and compute the time evolution via an integrated form of the transport equations, providing momentum and heat entrainment at the surface and at the bottom of the (uniform) mixed region. Thus, these 'bulk' type models do not allow for decaying or growing motions (e.g. the existence of vertical gradients) within a region of uniform density, even though this uniformity does not impose an instant constraint of velocity homogeneity in the region. A region made uniform by previous wind-stirring events can have strongly varying velocity gradients when subjected to future storms and turbulence build-up.

It was therefore natural to choose a 'profile' type model, for studying the time evolution of inertial shear and its statistics during a month-long simulation with time-varying momentum and heat fluxes. The particular profile model chosen was the Mellor–Yamada model with level 2.8 turbulence closure (MY2.8). This model was first introduced by Mellor and Yamada (1974) to study the turbulent planetary boundary layer, and later applied by Mellor and Durbin (1975) and Warn-Varnas and Piacsek (1979) to the oceanic mixed layer. A comparison of the level 2.0 and 2.5 closures for mixed layers was made by Martin (1985) at two weathership locations; he has also extended the level 2.5 closure to level 2.8.

We now give a brief description of the model. As all 'profile' or 'differential' type mixed-layer models, it uses the conservation equations for momentum, temperature, and salinity, defined on a finite-difference grid. In the momentum equations, the time and vertical spatial derivatives are retained, but the horizontal spatial derivatives are assumed to be small and are neglected. This implies, in particular, that horizontal pressure gradients are neglected. Vertical mixing is parameterized by using eddy coefficients computed via appropriate turbulence closure schemes corresponding to the level of closure of the Mellor–Yamada mixed-layer model. The MY2.8 model uses a critical Richardson number (Ri) cut-off criteria to suppress turbulence mixing in regions where the density stratification is large and the corresponding stability suppresses vertical motions. In this regard it is unlike the WP model (Warn-Varnas

and Piacsek, 1979), where the turbulence closure is of third order and does not involve a critical Ri cut-off of turbulence. Consequently, the WP model preserves the effects of shear penetration and of turbulence below the bottom of the mixed layer. The MY2.8 model, on the other hand, has no means of transferring momentum to depths below the mixed layer, because the cut-off mechanism has eliminated the existence of an eddy diffusion mechanism below the mixed layer.

The model is driven by surface fluxes of momentum, heat, and moisture. These fluxes can be derived from ship observations or from output of weather prediction models. As mentioned above, this model has been extensively tested at the weathership sites Papa (Station 'P') and November (Station 'N') by Martin (1985), and also for the location and duration of the MILE experiment (Davis et al., 1981; Warn-Varnas et al., 1981). In these cases the model was initialized from observed XBT profiles and driven using atmospheric surface fluxes derived from shipboard and/or buoy observations of the relevant physical variables.

The model has also been tested extensively in an operational setting at FNOC in Monterey, California, as part of the TOPS analysis/prediction system. In this case the temperature field is updated regularly by blending the predicted fields with analyzed fields that are a combination of climatology and recent XBT observations (Clancy and Martin, 1981; Clancy and Pollak, 1983). This operational model has predicted SST (sea-surface temperature) and MLD (mixed-layer depth) fields that had rms values much closer to the observed values than the corresponding climatological values.

For the particular model details, such as numerical schemes, turbulence closure and turbulence constants used in this study, the reader is referred to Martin (1985). We only want to add here that a rather small time step of 300 s was necessary to run the case with $\delta z = 1$ m, and to keep the comparisons meaningful the same time step was used for all vertical grid spacings.

5

Initialization and forcing

The simulations were initialized from climatological temperature and salinity profiles, in particular by the fields of the GDEM (Generalized Digital Environmental Model) climatology (Naval Oceanographic Office, 1987). The mixed-layer model was then driven by wind stresses and heat fluxes derived from observations of the relevant atmospheric and oceanic variables by the weathership 'Mike' stationed in the Norwegian Sea at 66°N, 2°E for the years 1960–1979 (Martin, personal communication, 1987). Solar radiation, infrared back-radiation, and evaporative and sensible surface heat flux components were individually given, as well as the total net surface heat flux. Penetration of solar radiation was described using an extinction profile for seawater optical type 2 (Jerlov, 1976).

Figures 1–3 show the time variation of the surface wind stress for 12 years of the 20-year period employed in this study (1960–1979). Within this 20-year period, the May winds showed a remarkably uniform average of 0.10–0.15 dynes/cm². The winds fluctuated almost regularly with a period of 3–4 days, with the stresses varying from nearly 0.0 to 0.4 dynes/cm². Some of the more prominent events are three exceptionally large storms that occurred in the Mays of 1964, 1965 and 1975, respectively. Two short periods of intense winds also occurred in May 1978, and some lesser storms in 1966, 1976 and 1979.

The simulations were actually started on April 15 of each year, to provide a necessary 'spin-up' of the model in order to achieve dynamical balance on the starting date of the statistical analysis, i.e. May 1 of each year.

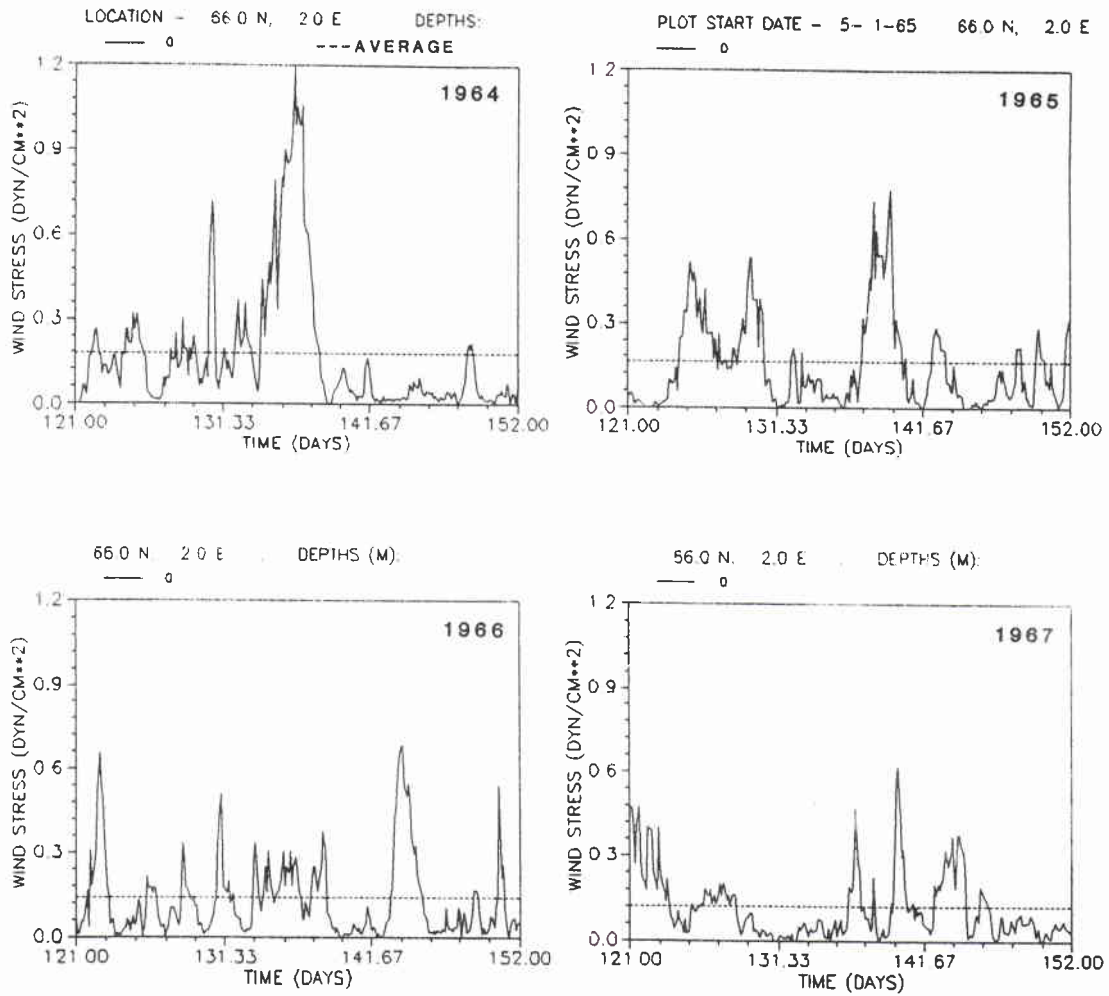


Figure 1 Daily variation of the scalar wind stress during the month of May in the years 1964-67, at the weather ship 'Mike' location (66°N, 2°E).

SACLANTCEN SM-241

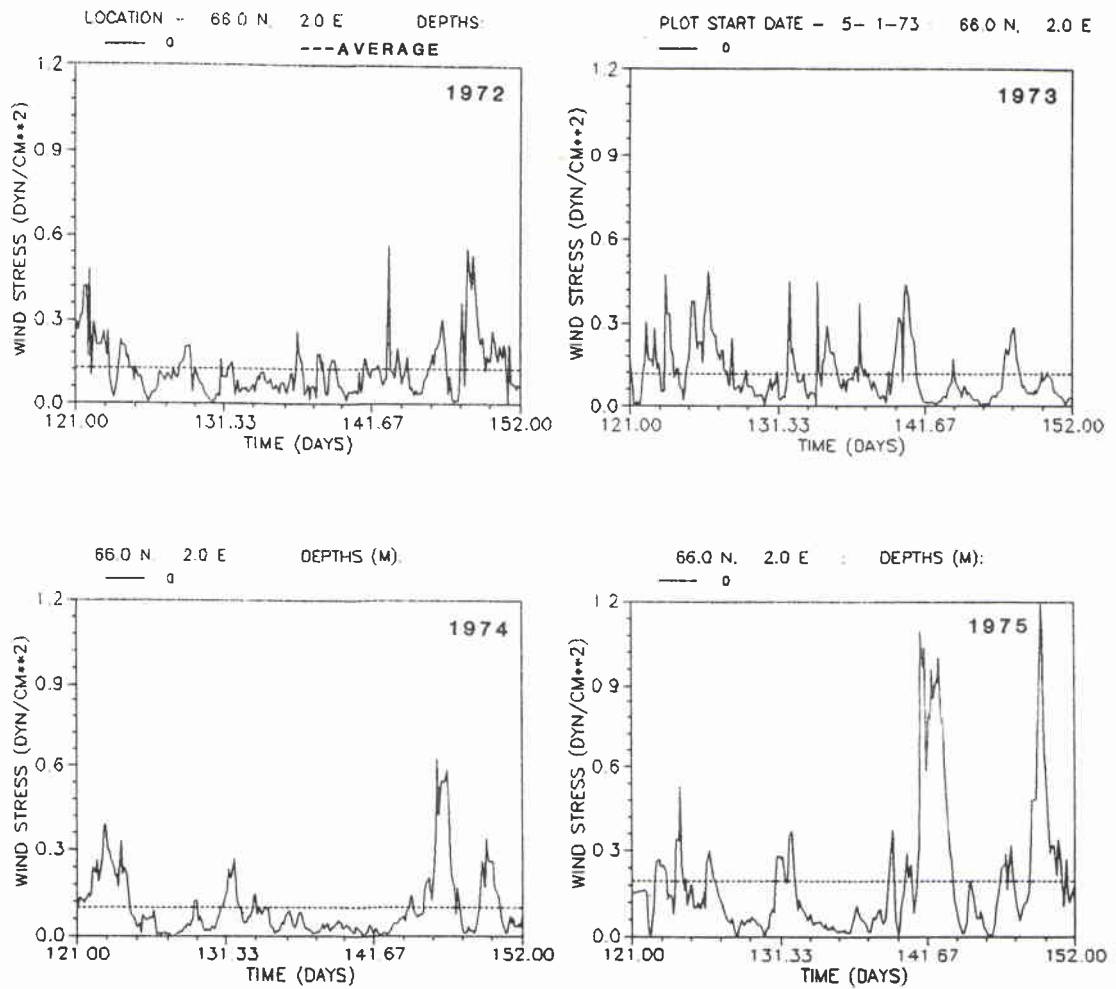


Figure 2 Daily variation of the scalar wind stress during the month of May in the years 1972-75, at the weathership 'Mike' location (66°N,2°E).

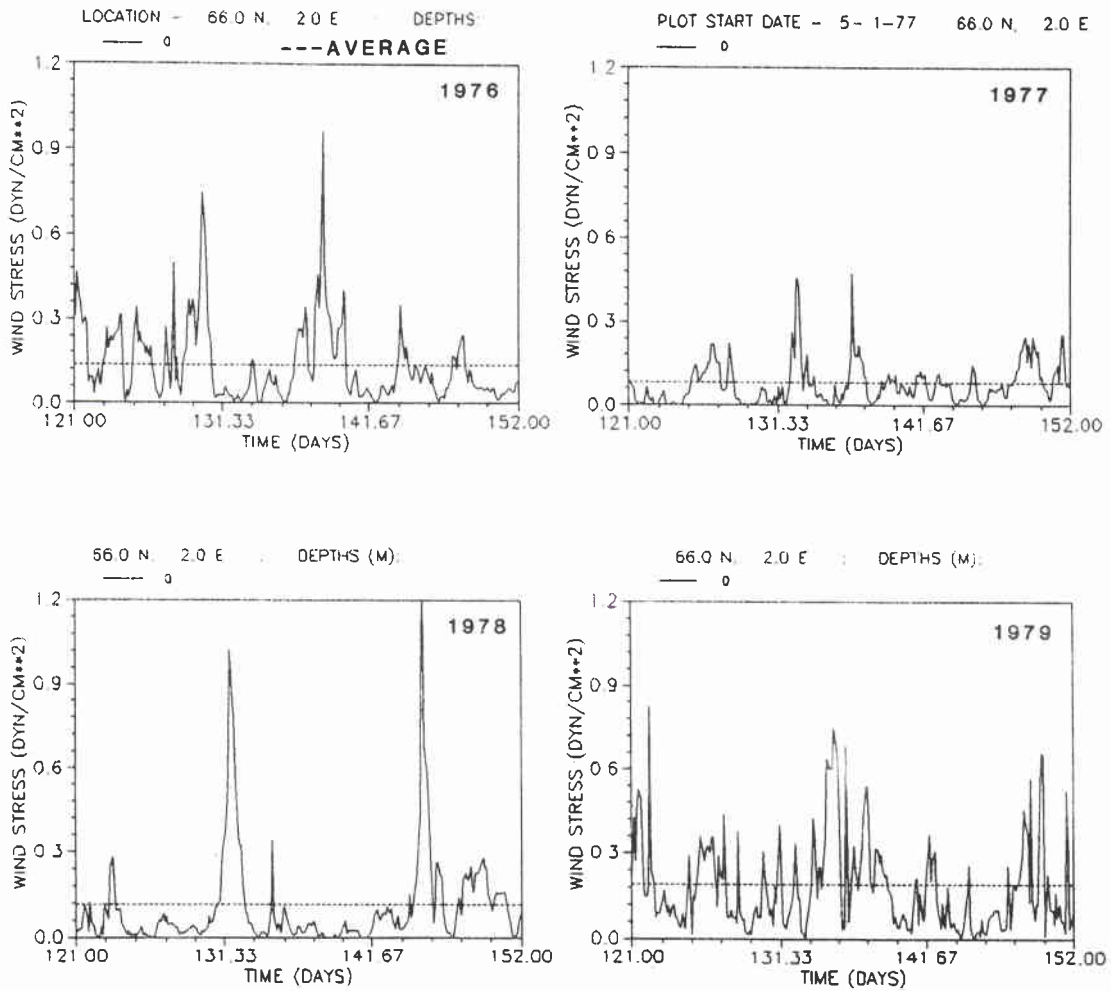


Figure 3 Daily variation of the scalar wind stress during the month of May in the years 1976-79, at the weather ship 'Mike' location (66°N, 2°E).

Statistical method and output display

We have been mainly interested in the behavior of the scalar shear S , defined as

$$S = ((\partial u / \partial z)^2 + (\partial v / \partial z)^2)^{1/2},$$

where u and v are the x and y (north and east) components of velocity, and δz represents the vertical distance between grid points. The values of S were calculated every 6 h from the velocities at the various grid levels.

We have computed both averages and rms values of the scalar shear over the months of May for each year of the 20-year period from 1960–1979. The mean values were obtained by averaging 120 values (four times a day) of each May, for each depth level and each year, respectively. These were then plotted as a series of vertical profiles for the different years. The rms values were first sorted into depth bins of 10-m width (from 0 to 100 m), and then also into magnitude bins of width 10^{-3} s^{-1} , with the total ranging from 0 to 10^{-2} s^{-1} . From these we have constructed 2-D plots of shear magnitude *vs* depth, for each year and each computational grid. We have also prepared 3-D statistical plots that display the frequency of occurrence of shear as a function of depth and magnitude of shear. However, because of the excessive details and, to some extent, repetitiousness of the plots, only a 15-year average of the 3-D histograms is presented for each of the four grids used, i.e. for constant grids with $\delta z = 1, 2, \text{ and } 5 \text{ m}$, and the TOPS grid (a stretched grid whose initial grid size near the surface is 5 m).

7

Discussion of results

The internal grid spacing was found to have a profound effect on shear statistics, as displayed in both the depth profiles and the 2-D and 3-D histograms. Figures 4 and 5 present the monthly mean shear profiles as a function of year for three model grid sizes used, $\delta z = 1, 2,$ and 5 m, respectively. Each figure contains 12 profiles, representing four successive years (1970–73) at the three model resolutions.

It is evident from the figures that the mean shear profiles vary more with grid size than with the years. Generally, it can be said that smaller grid sizes lead to ‘spikier’ or ‘sharper’ shear maxima. Furthermore, somewhat surprisingly, the mean shears tend to increase with grid size over the whole depth domain, and penetrate further down into the seasonal thermocline. Whereas in the 1-m simulation the maxima near the bottom of the mixed layer occur between 30 and 60 m, in the 5-m simulation the maxima tend to occur between 60 and 80 m. This apparent increase in MLD with grid spacing can at least partly be explained by the criterion used for finding the MLD, namely the depth at which the temperature (or density) has fallen a certain prescribed increment below its surface value. Since in general this depth might fall between two grid points, and the criterion then ascribes the MLD to the deeper of the points, the larger grids will tend to have the deeper MLD.

In greater detail, the 1-m profiles display about two or three local maxima or ‘peaks’ that reflect the presence of large ‘bottom-of-the-mixed-layer’ shear events. Unfortunately, there is no clear-cut trend as to how the shifting and growth of these peaks occurs with changing grid size. For example, in 1976 the three peaks appearing at 24, 44 and 56 m in the 1-m simulations have shifted to 26, 60, and 80 m, respectively, in the 2-m simulations. In the 5 m simulations, they have almost lost their ‘spiky’ character, with only some local maxima visible at 80 and 48 m, and two larger peaks at 8 and 28 m. Whereas in both the 1- and 2-m simulations the peak magnitudes increased with depth, in the 5-m simulations the reverse is found to be true. The tendency to form peaks at the surface with increasing δz is clearly evident for almost all years. Furthermore, the penetration of shear to lower depths for increasing grid spacing is also evident: the effective penetration depth is ca. 65 m for the 1-m simulations and ca. 100 m for the 5-m simulations.

It must be pointed out that although the statistics of shear presented here are probably valid from the surface to the bottom of the mixed layer, they are not valid below the mixed layer. As discussed above, comparisons of the MY2 model to data at MILE showed that although the model simulated physical parameters well within

SACLANTCEN SM-241

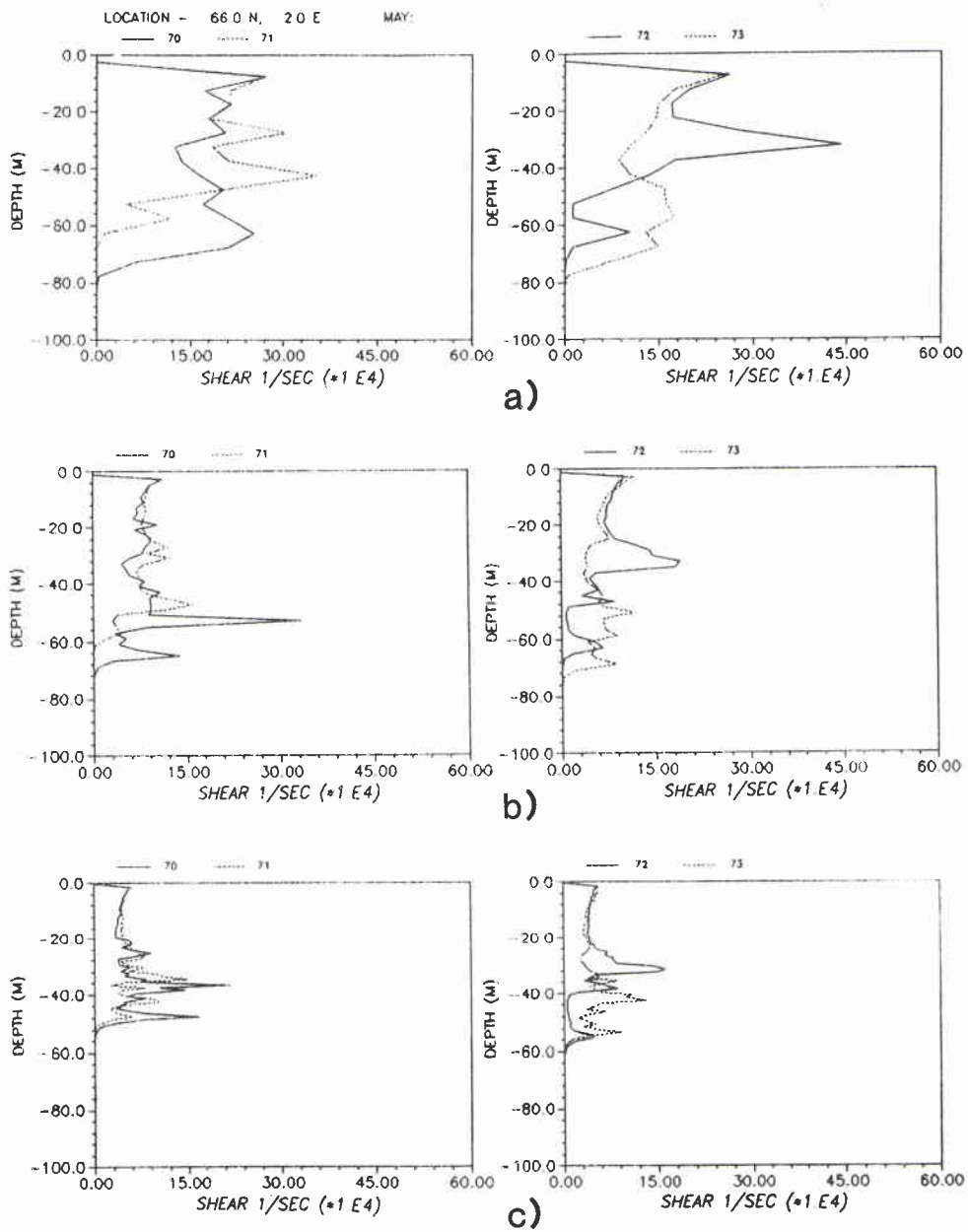


Figure 4 Variation of the monthly mean shear profiles with year and the vertical model grid spacing, in the years 1970–73: (a) $\delta z = 5$ m, (b) $\delta z = 2$ m, (c) $\delta z = 1$ m. The left column is for the years 1970, 1971, the right column for the years 1972, 1973.

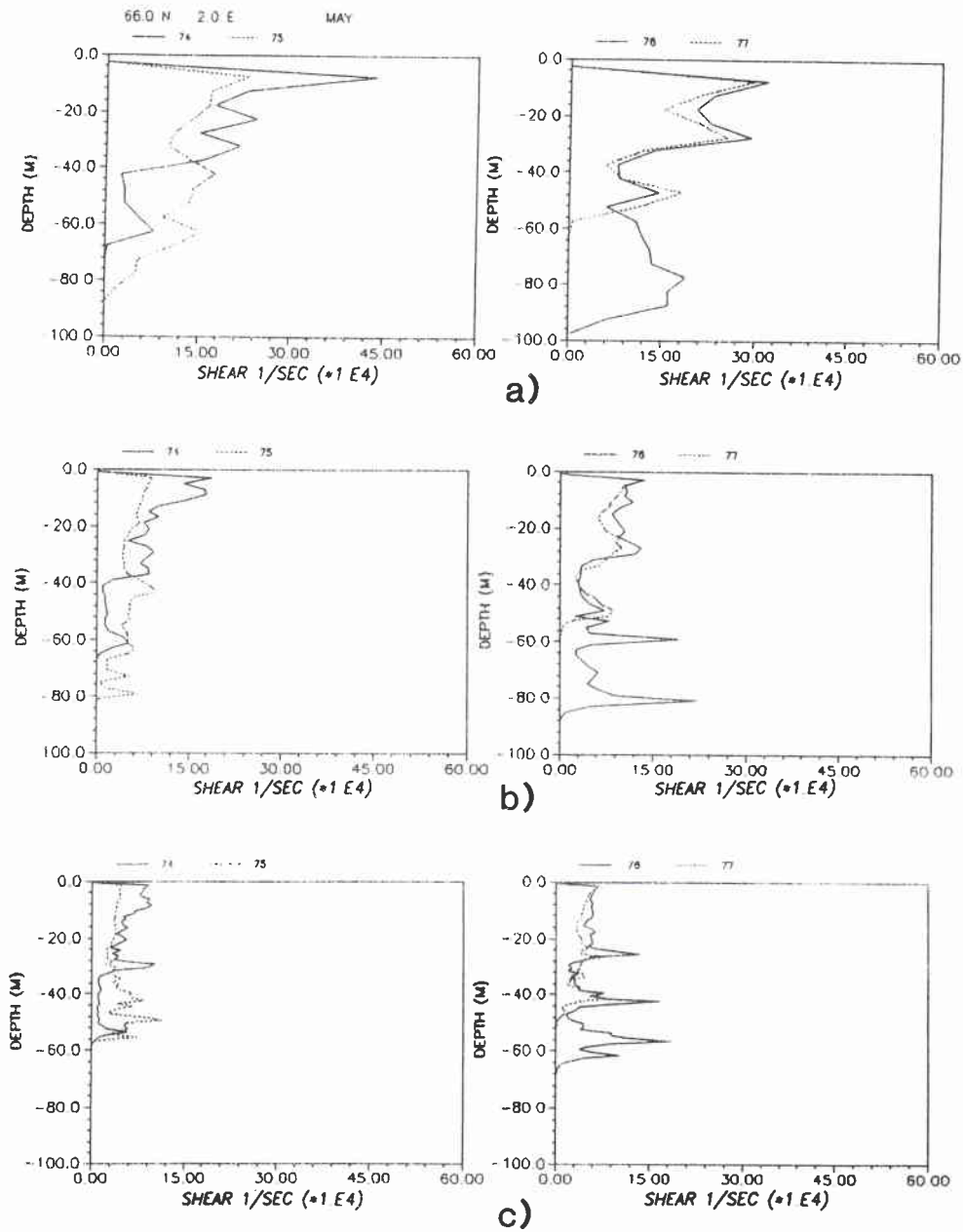


Figure 5 Variation of the monthly mean shear profiles with year and the vertical model grid spacing, in the years 1974-77: (a) $\delta z = 5$ m, (b) $\delta z = 2$ m, (c) $\delta z = 1$ m. The left column is for the years 1974, 1975, the right column for the years 1976, 1977.

the mixed layer, below the mixed layer there was much more shear than the model showed.

The absence of shear at the $\delta z = 0$ m grid point on all profiles is an artifact, because there was no zero-point output from the model. In fact, the shear values can be seen to approach a local maximum at the first grid point below the surface.

The 15-year average behavior of shear (1964–80) is illustrated in the 3-D histogram plots of Fig. 6 as a function of the four computational grids used, respectively. The histograms display a probability distribution for the occurrence of a given shear magnitude at a given depth. According to these results, the largest shears tend to occur near the surface. A secondary local maximum, only slightly smaller than the surface value, is evident in all except the 5-m simulations, at ca. 40 m in the 1- and 2-m simulations, and at ca. 60 m for the TOPS grid results. There occur almost no shear values above $2 \times 10^{-3} \text{ s}^{-1}$ in the 1- and 2-m simulations, but ca. 10% or more of the shear values fall into the $3\text{--}4 \times 10^{-3} \text{ s}^{-1}$ range in the 5-m and the TOPS simulations. These ratios of occurrences between the large and small shear values are approximately the same at all the depth levels examined. Another interesting feature is the rather abrupt cut-off of shear below a certain critical depth, at ca. 65 m for the 1-m simulations and ca. 85 m for the 2-m simulations. The fall-off with depth appears to be almost exponential for the TOPS grid, but for the 5-m simulation a second local maximum is found at 100 m.

The effect of grid size on shear output is more obvious on shear *vs* depth profile plots (Fig. 3) than in the histogram plots (Figs. 4–7) because different numbers of points were grouped together into 10-m ‘bins’ for each grid size: for the 1-m grid, ten points were grouped together for each 10-m box representing a range step, for the 2-m grid, five points were grouped together, and for the 5-m grid, only two points. This use of ‘bins’ results in a smoothing effect.

The behavior of the mean shear and its rms deviation in the two consecutive decades 1960–69 and 1970–79 is depicted in Fig. 7, respectively, again as a function of the vertical grid size. This figure is actually a 2-D version of the 3-D histogram-functions presented in Fig. 6, representing the 10-m average shear with depth (obtained by integrating the values in each 10-m bin in Fig. 6 over all magnitudes).

Two overall trends for the mean shear can be distinguished: the slightly sharper cut-off of the mean shear with depth during the ‘60s *vs* the ‘70s (left *vs* right column in Fig. 7), and the sharper cut-off with finer grid resolution (top, 5 m; center, 2 m; bottom, 1 m – in Fig. 7).

Figures 8 and 9 depict the annual variation of the rms deviation in the decade 1960–69, for the years 1960–61 and 1962–63, respectively. The deviations are computed for three model grid resolutions. Similar results were obtained by comparing the rms deviation between single years and the 10-year average for the decade 1970–79.

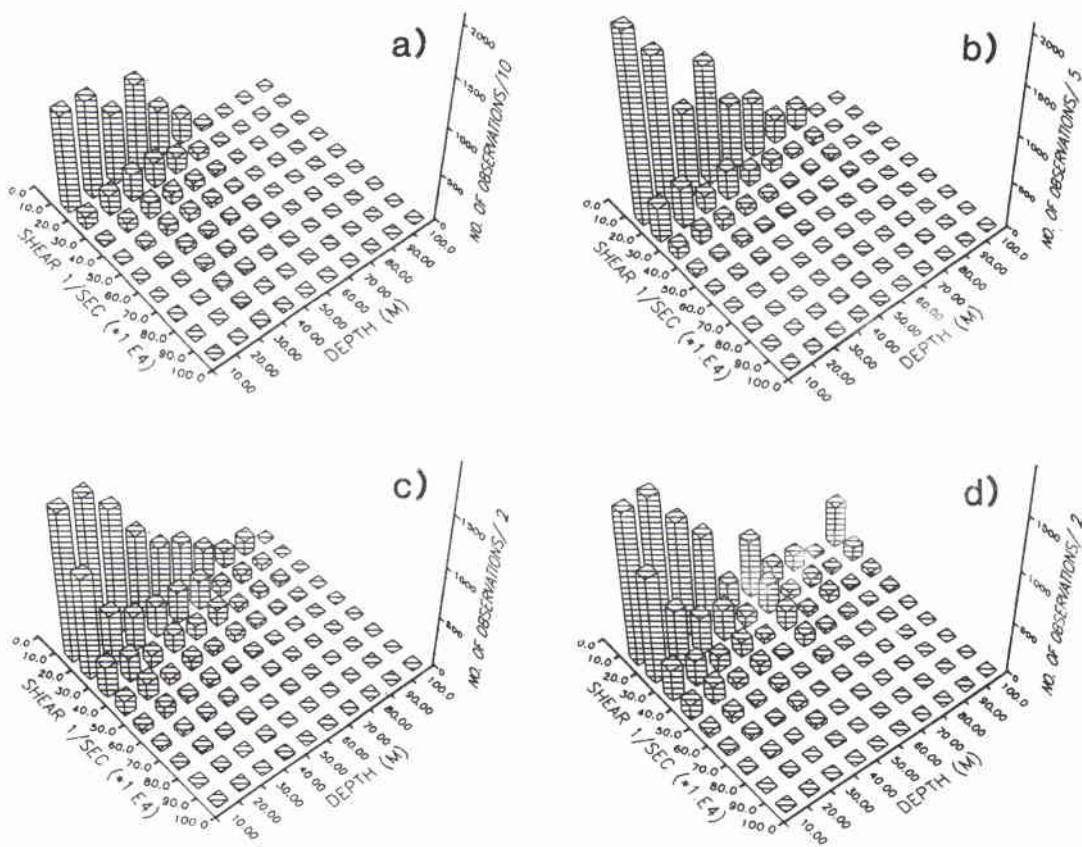


Figure 6 Probability distribution of the 15-year average shear with depth and magnitude, as a function of model grid spacing: (a) $\delta z = 1$ m, (b) $\delta z = 2$ m, (c) $\delta z = 5$ m, (d) TOPS stretched grid with surface $\delta z = 2.5$ m.

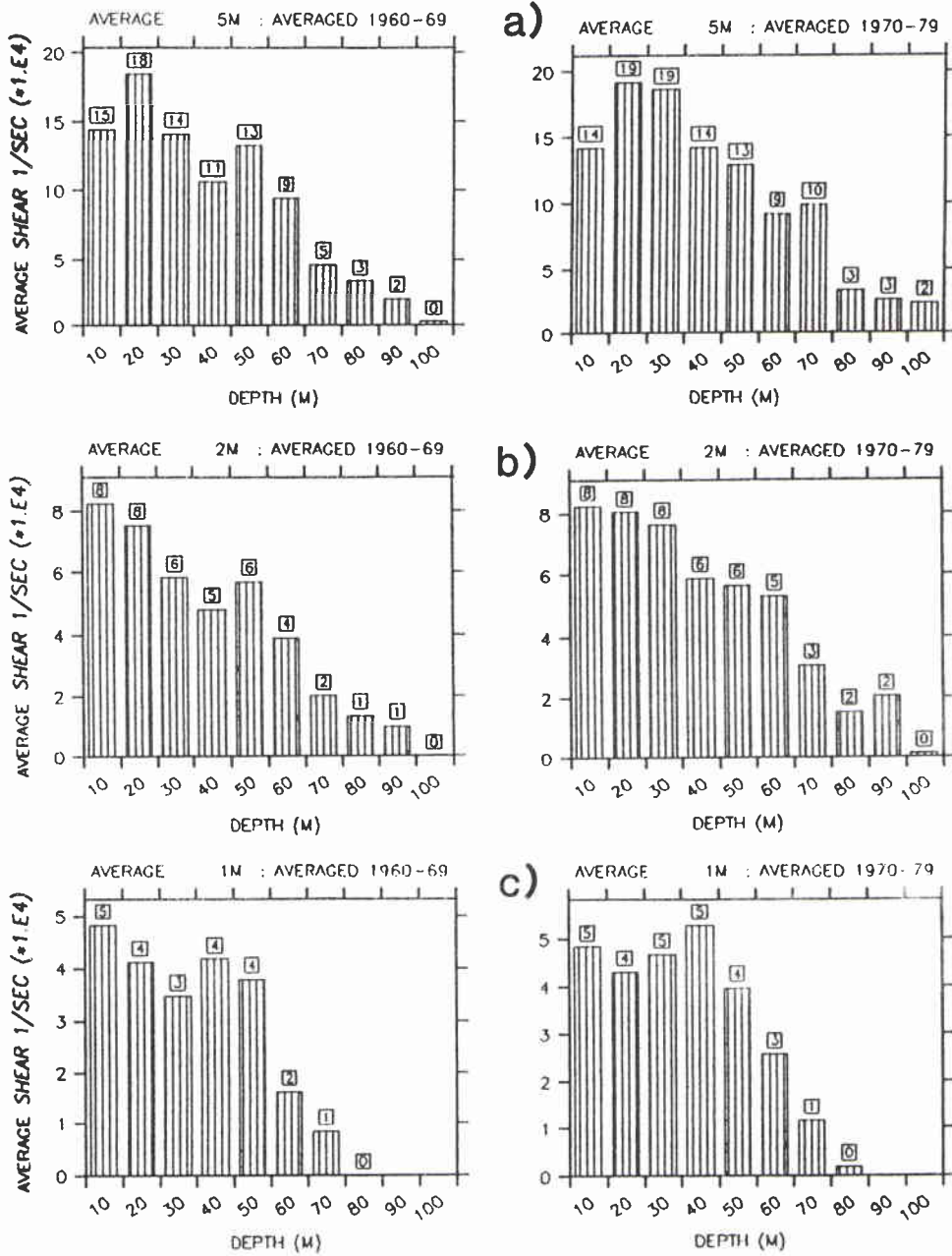


Figure 7 Distribution in 10-m 'bins' of the 10-year average shear with depth and magnitude, as a function of model grid spacing and decade of averaging: (a) $\delta z = 5$ m, (b) $\delta z = 2$ m, (c) $\delta z = 1$ m. The left column is for the decade 1960-69, and the right column is for the decade 1970-79.

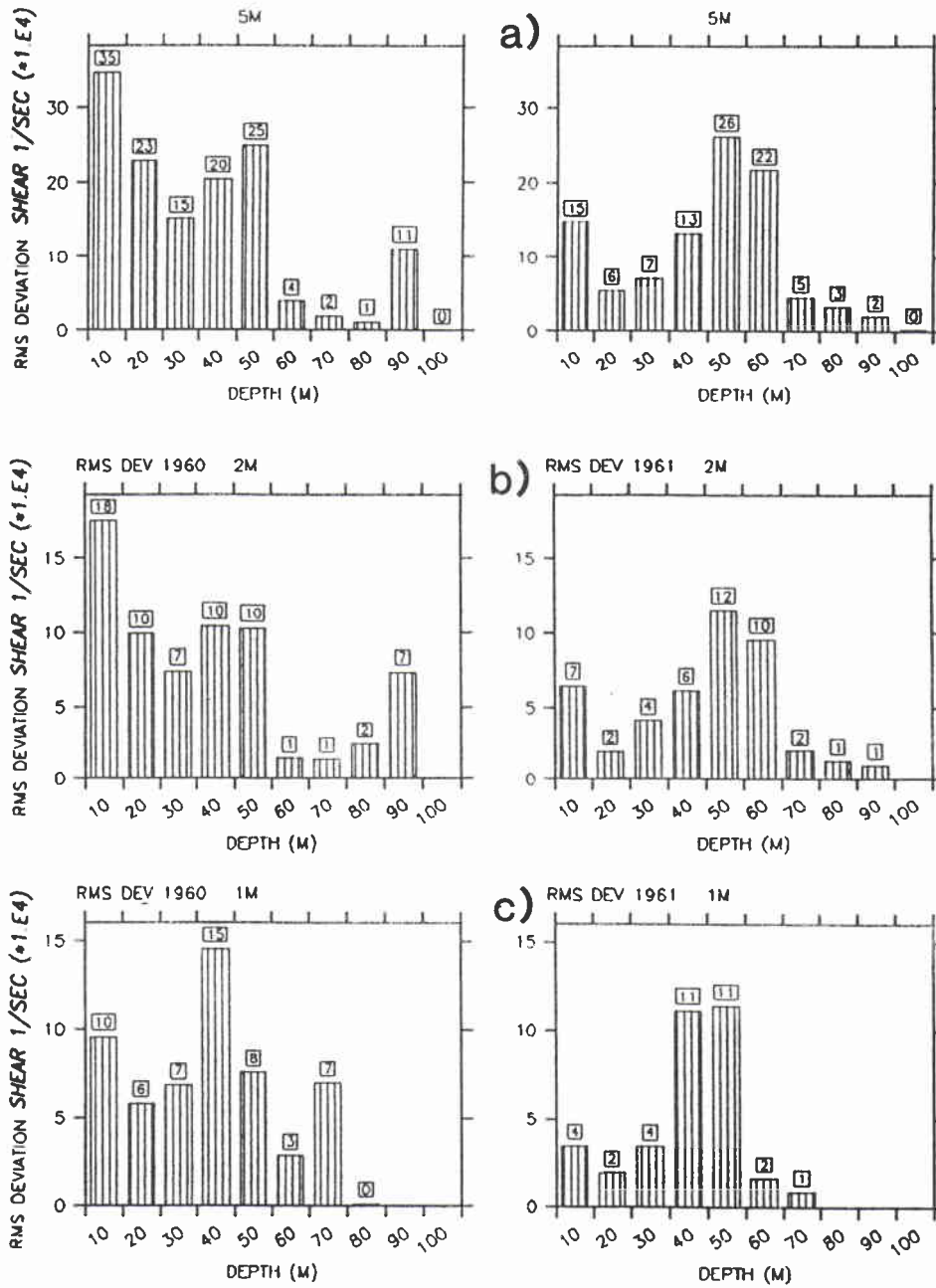


Figure 8 Distributions in 10-m 'bins' of the monthly average rms shear variability with depth and magnitude, as a function of model grid spacing and year: (a) $\delta z = 5$ m, (b) $\delta z = 2$ m, (c) $\delta z = 1$ m. The left column is for the year 1960, and the right column is for the year 1961.

SACLANTCEN SM-241

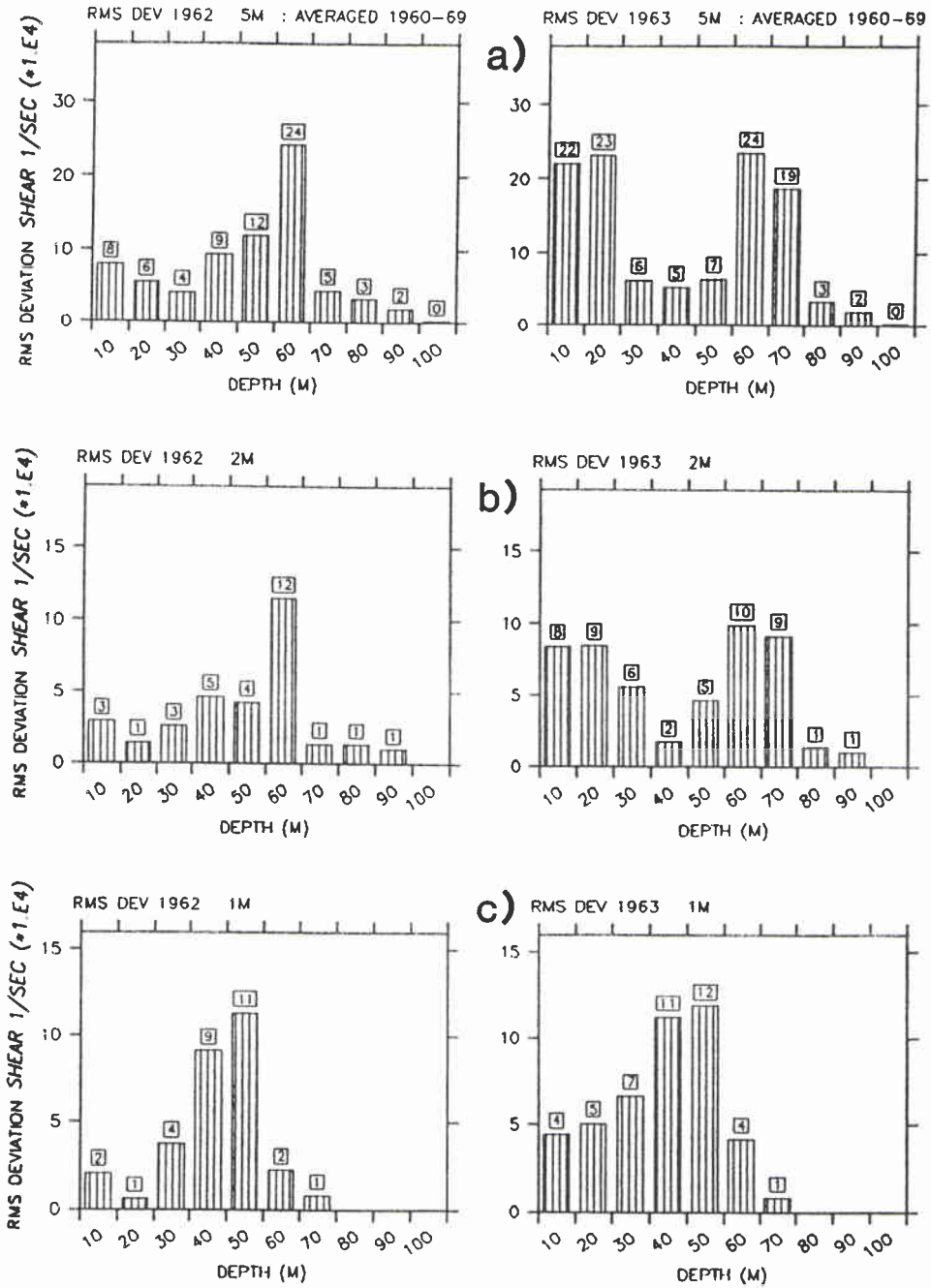


Figure 9 Distributions in 10-m 'bins' of the monthly average rms shear variability with depth and magnitude, as a function of model grid spacing and year: (a) $\delta z = 5$ m, (b) $\delta z = 2$ m, (c) $\delta z = 1$ m. The left column is for the year 1962, and the right column is for the year 1963.

There appear to be significant interannual variations as well as a grid dependence of the fluctuations. For all grid sizes, the largest interannual changes are between 1960 and 1961; particularly noteworthy is the presence of very strong surface shear in 1960, and its almost complete absence in 1962. In all years the largest deviations occur below the surface, in the 40–50 m depth range for the 1-m results, and in the 50–70 m depth range for the 2 and 5 m simulations. The magnitude and depth range of this subsurface peak are almost constant from 1961 to 1963 in the 1-m simulation, but there is a tendency to drift to a deeper depth in the coarser grid results, from ca. 55 m in 1961 to ca. 65 m in 1963. In general, the subsurface peak spans a depth range of ca. 20 m in all four years and for all grid resolution, except in 1962 for the 2- and the 5-m results, when it is only ca. 10 m wide.

8

Conclusions

We have observed a strong dependence of the vertical inertial shear on model grid size and annual variations in the forcing. Both dependencies are enhanced by the nonlinear nature of the mixing processes, e.g. a cubic dependence on the wind speed and a quadratic dependence on shear and stability gradients (δz^{-2}) in the Richardson number. In general, the 1-m grid results differ substantially from the 2- and 5-m results, which are on the whole similar. The TOPS results tend to agree with the 2-m results near the surface, with the 5-m results above 60 m, and diverge from all below that depth, reflecting the stretched nature of its model grid.

References

- D'Asaro, E. and Sanford, T.B. STREX upper ocean velocity profiles. In 'Storm Transfer and Response Experiment' workshop report, Washington, D.C., US Dept. of Commerce, 1981.
- Briscoe, M.G. and Weller, R.A. Preliminary results from the long-term upper-ocean study (LOTUS). *Dynamics of Atmospheres and Oceans*, **8**, 1984: 243-265.
- Clancy, R.M. and Martin, P.J. Synoptic forecasting of the oceanic mixed layer using the Navy's operational environmental data base: Present capabilities and future applications. *Bulletin of the American Meteorological Society*, **62**, 1981: 770-784.
- Clancy, R.M. and Pollak, K.D. A real-time synoptic ocean thermal analysis/forecast system. *Progress in Oceanography*, **12**, 1983: 383-424.
- Clancy, R.M., Martin, P.J., Piacsek, S.A. and Pollak, K.D. Test and evaluation of an operationally capable synoptic upper-ocean forecast system, NORDA TN #92. NSTL, MS, Naval Ocean Research and Development Activity, 1981. [AD A 098 908]
- Davis, R.E., DeSzoeki, R., Halpern, D. and Niiler, P. Variability in the upper ocean during MILE. Part I: The heat and momentum balances. *Deep Sea Research*, **28A**, 1981a: 1427-1451.
- Davis, R.E., DeSzoeki, R. and Niiler, P. Variability in the upper ocean during MILE. Part II: Modeling the mixed-layer response. *Deep Sea Research*, **28A**, 1981b: 1453-1475.
- Garrett, C.J. and Munk, W.H. Space-time scales of internal waves. *Geophysical Fluid Dynamics*, **2**, 1972: 225-264.
- Garrett, C.J. and Munk, W.H. Space-time scales of internal waves, a progress report. *Journal of Geophysical Research*, **80**, 1975: 291-297.
- Gregg, M.C. and Sanford, T.B. Signatures of mixing from the Bermuda slope, the Sargasso Sea and the Gulf Stream. *Journal of Physical Oceanography*, **10**, 1980: 105-127.
- Harding, J.M., Preller, R.H. and Piacsek, S.A. Statistics of vertical shear from a global model, NORDA TN #206. NSTL, MS, Naval Ocean Research and Development Activity, 1983.
- Jerlov, N.G. *Marine Optics*. Amsterdam, Elsevier, 1976.
- Levine, M.D., DeSzoeki, R.A. and Niiler, P.P. Internal waves in the upper ocean during MILE. *Journal of Physical Oceanography*, **13**, 1983: 240-257.
- Naval Oceanographic Office, Data Base, Description for Master Generalized Digital Environmental Model (GDEM), Commanding Officer, Naval Oceanographic Office, Bay St. Louis, NSTI MS 39522-5001.
- Martin, P.J. Mixed-layer simulation of buoy observations taken during Hurricane Eloise. *Journal of Geophysical Research*, **87**, 1982: 409-427.
- Martin, P.J. Simulation of the mixed layer at OWS November and Papa with several models. *Journal of Geophysical Research*, **90**, 1985: 903-916.

SACLANTCEN SM-241

Martin, P.J., Warn-Varnas, A.C., French, J.P. and Piacsek, S.A. Comparison of model-predicted shear with observations during MILE, NORDA TN328. NSTL, MS, Naval Ocean Research and Development Activity, 1986.

Mellor, G.L. and Yamada, J. A hierarchy of turbulence closure models for planetary boundary layers. *Journal of the Atmospheric Sciences*, **31**, 1974: 1791-1806.

Mellor, G.L. and Durbin, P.A. The structure and dynamics of the ocean surface mixed layer. *Journal of Physical Oceanography*, **5**, 1975: 718-728.

Oakey, N.S. Determination of the rate of dissipation of turbulent energy from simultaneous temperature and velocity shear microstructure measurements. *Journal of Physical Oceanography*, **12**, 1982: 256-271.

Oakey, N.S. and Elliott, J.A. Dissipation within the surface mixed layer. *Journal of Physical Oceanography*, **12**, 1982: 171-185.

Piacsek, S.A., Henderson, L., Van Meurs, P., Warn-Varnas, A.C. and French, J.P. Operational prediction of upper ocean environmental parameters. Part 1: Analysis of TOPS output, NORDA TN #379. NSTL, MS, Naval Ocean Research and Development Activity, 1988.

Pinkel, R. Doppler sonar observations of internal waves: The wavenumber-frequency spectrum. *Journal of Physical Oceanography*, **14**, 1984: 1249-1270.

Preller, R.H. and Piacsek, S.A. Vertical shear from TOPS, NORDA TN #300. NSTL, MS, Naval Ocean Research and Development Activity, 1985.

Rubenstein, D.M. and Newman, F.C. Statistical analysis of upper ocean time series of vertical shear, Science Applications, Inc. TR SAI-83-751-WA. Arlington, VA, 1982. [AD A 117 286]

Warn-Varnas, A.C. and Piacsek, S.A. An investigation of the importance of third-order correlations and choice of length scale in mixed layer modelling. *Geophysical and Astrophysical Fluid Dynamics*, **13**, 1979: 225-243.

Warn-Varnas, A.C., French, J.P., Piacsek, S.A., Martin, P.J. and Harding, G. Real-time shear predictions, NORDA TN #307. NSTL, MS, Naval Ocean Research and Development Activity, 1986.

Warn-Varnas, A.C., Dawson, G.M. and Martin, P.J. Forecast and studies of the oceanic mixed-layer during the MILE experiment. *Geophysical and Astrophysical Fluid Dynamics*, **17**, 1981a: 63-85.

Warn-Varnas, A.C. and Dawson, G. An analysis of modeled shear distribution during MILE, NORDA TN #84. NSTL, MS, Naval Ocean Research and Development Activity, 1981b.

Initial Distribution for SM-241

<u>SCNR for SACLANTCEN</u>		<u>National Liaison Officers</u>	
SCNR Belgium	1	NLO Canada	1
SCNR Canada	1	NLO Denmark	1
SCNR Denmark	1	NLO Germany	1
SCNR Germany	1	NLO Italy	1
SCNR Greece	1	NLO Netherlands	1
SCNR Italy	1	NLO UK	1
SCNR Netherlands	1	NLO US	4
SCNR Norway	1		
SCNR Portugal	1		
SCNR Spain	1		
SCNR Turkey	1	Total external distribution	26
SCNR UK	1	SACLANTCEN Library	10
SCNR US	2	Stock	24
SECGEN Rep. SCNR	1		
NAMILCOM Rep. SCNR	1	Total number of copies	60